Cell-free mixing of *Escherichia coli* crude extracts to prototype and rationally engineer high-titer mevalonate synthesis

Quentin M. Dudley[1], **Kim C. Anderson**[1], **Michael C. Jewett**[1,2,3,4,*]

[1]Department of Chemical and Biological Engineering, Northwestern University, Evanston, IL 60208, USA,

[2]Chemistry of Life Processes Institute, Northwestern University, Evanston, IL 60208, USA,

[3]Robert H. Lurie Comprehensive Cancer Center, Chicago, IL 60611, USA

[4]Simpson Querrey Institute Northwestern University, Chicago, IL 60611, USA

Abstract

Cell-free metabolic engineering (CFME) is advancing a powerful paradigm for accelerating the design and synthesis of biosynthetic pathways. However, as most cell-free biomolecule synthesis systems to date use purified enzymes, energy and cofactor supply can be limiting. To address this challenge, we report a new CFME framework for building biosynthetic pathways by mixing multiple crude lysates, or extracts. In our modular approach, cell-free lysates, each selectively enriched with an overexpressed enzyme, are generated in parallel and then combinatorically mixed to construct a full biosynthetic pathway. Endogenous enzymes in the cell-free extract fuel high-level energy and cofactor regeneration. As a model, we apply our framework to synthesize mevalonate, an intermediate in isoprenoid synthesis. We use our approach to rapidly screen enzyme variants, optimize enzyme ratios, and explore cofactor landscapes for improving pathway performance. Further, we show that genomic deletions in the source strain redirect metabolic flux in resultant lysates. In an optimized system, mevalonate was synthesized at 17.6 g·L^{-1} (119 mM) over 20 hours, resulting in a volumetric productivity of 0.88 g·L^{-1}·hr^{-1}. We also demonstrate that this system can be lyophilized and retain biosynthesis capability. Our system catalyzes ~1250 turnover events for the cofactor NAD$^+$ and demonstrates the ability to rapidly prototype and debug enzymatic pathways *in vitro* for compelling metabolic engineering and synthetic biology applications.

Keywords

cell-free metabolic engineering; metabolic pathway debugging; cell-free synthetic biology; mevalonate; *Escherichia coli*; *in vitro*

Isoprenoids are a promising class of metabolic engineering targets with over 40,000 known structures and potential uses as pharmaceuticals, flavors, fragrances, pesticides,

*****Correspondence**: Michael C. Jewett, Department of Chemical and Biological Engineering, Northwestern University, Evanston, IL 60208, USA, m-jewett@northwestern.edu, **Tel**: 1 847 467 5007; **Fax**: 1 847 491 3728.

disinfectants, and chemical feedstocks.[1, 2] Already, the field has demonstrated heterologous production of the anti-malarial drug artemisinin,[3] the anti-cancer compound intermediate taxadiene,[4] the rubber-precursor isoprene,[5] the ginkgolide-precursor levopimaradiene,[6] the commodity chemical limonene,[7] the biofuel 3-methyl-3-buten-1-ol,[8] and many other plant secondary metabolites.[9, 10]

While the number[11] and impact[12–14] of industrial-scale metabolic engineering processes is increasing, engineering biosynthetic pathways within cells remains subject to several constraints. First, delicate flux balancing and promoter tuning can be time-consuming. [4, 15–17] In one example, the semi-synthetic artemisinin endeavor required over 150 person-years of work, mostly for "pathway balancing".[12] Second, cell viability is often limited by the high concentrations of intermediate metabolites or final products.[18] A specific challenge for isoprenoid production using the mevalonate pathway (Figure 1A) is the build-up of the toxic intermediate hydroxymethylglutaryl (HMG)-CoA.[19, 20] Finally, competition between the cell's physiological and evolutionary objectives (growth) and the engineer's process objectives (target production) can result in low volumetric productivities ($g \cdot L^{-1} \cdot hr^{-1}$) and byproduct loses through competing pathways.[21] Due to these constraints, new prototyping tools and biomanufacturing strategies are needed to alleviate long development times and facilitate faster pathway optimization.[22]

In recent years, cell-free metabolic engineering (CFME) has emerged as a new approach to prototype pathway performance and expand the paradigm of traditional biomanufacturing. [21–26] CFME employs *in vitro* ensembles of catalytic proteins for the production of target products.[22] Cell-free systems permit easy manipulation of reaction conditions, avoid possible toxicity constraints, and theoretically allow all carbon/energy resources to be directed to product formation. While purified enzyme systems offer exquisite control of reaction components,[27–30] crude lysates contain highly active and complex metabolic networks without the need for purification. The ability of crude extracts to recycle energy and cofactors highlights a key advantage of lysate-based CFME. For example, previous demonstrations of crude lysate CFME for production of dihydroxyacetone phosphate (DHAP) derivatives,[31] ethanol,[32] and 2,3-butanediol[33] highlight long (>8 enzyme) pathways with high cofactor turnover. However these examples all used lysates created from a single source strain containing the entire metabolic pathway.

Here we propose a new approach for crude extract-based CFME. Specifically, we sought to re-conceptualize the "build" step of design-build-test loops by advancing a modular approach to making molecules using cell-free cocktails containing multiple lysates (or extracts). The key idea is that each enzyme in the candidate pathway is overexpressed in its own source strain, from which an extract is prepared. Then, the extracts are mixed in multiple, different ratios to assemble the pathway and provide initial insights into beneficial enzyme ratios, promiscuity to different starting substrates, and possible side reactions. This work builds on efforts by Liu *et al.* to prototype fatty acid biosynthesis using purified enzymes plus a single lysate,[34] however, in our approach the enzymes are not purified. We validated this concept by prototyping a system for conversion of glucose to mevalonate, an intermediate in isoprenoid synthesis (Figure 1B).

We show that our method provides flexibility for rapidly testing enzyme variants, manipulating physicochemical conditions, and assessing genomic modifications on pathway performance. We expect the methods reported here to provide a discovery-centered strategy for assessing biosynthetic pathway in a system that (i) mimics the cytoplasmic environment, (ii) permits design-build-test (DBT) iterations without the need to reengineer organisms, and (iii) explores combinatorial and modular assembly of pathways through the use of well-defined experimental conditions. As previous publications have shown that enzymes selected for *in vitro* activity subsequently perform well in the cell,[34–39] our approach may aid in the development of enzyme pathways and perhaps circuits[40–42] for metabolic engineering and synthetic biology applications. Our work may also advance interest in using CFME systems for biomanufacturing[22].

Results and Discussion

Construction of a cell-free platform for mevalonate production

To demonstrate our new framework for CFME, we selected the mevalonate synthesis pathway.[43] The goal was to reconstruct mevalonate biosynthesis *in vitro* by mixing and matching selectively enriched lysates in cell-free cocktails. Endogenous enzymes for central metabolism in the lysate would catalyze the native glycolytic cascade from glucose to acetyl-CoA, which was coupled with three overexpressed enzymes to convert acetyl-CoA to mevalonate (Figure 1A). Previous efforts have shown that *E. coli* crude extracts have highly active central metabolism[44] and are able to rapidly metabolize glucose to pyruvate, acetyl-CoA, and other glycolytic intermediates.[31, 33]

To enable cell-free biosynthesis of mevalonate, we first introduced individual genes into the source strain BL21(DE3). These genes encode one of three enzymes needed to convert acetyl-CoA to mevalonate (See Table 1 for Strains and Plasmids and Appendix S1 for gene sequences). The three enzymes and their functions are described here. First, acetyl-CoA acetyltransferase (ACAT) catalyzes a Claisen condensation of two acetyl-CoA molecules to acetoacetyl-CoA. Second, hydroxymethylglutaryl-CoA synthase (HMGS) mediates the condensation of acetyl-CoA with acetoacetyl-CoA to generate 3-hydroxy-3-methyglutaryl-CoA (HMG-CoA). Third, hydroxymethylglutaryl-CoA reductase (HMGR) facilitates a four-electron oxidoreduction of HMG-CoA to mevalonate requiring two NADPH or two NADH. [45] Separate crude lysates of *E. coli* BL21(DE3), each overexpressing a single pathway enzyme (ACAT, HMGS, or HMGR), were prepared. Based on our previous work,[33] we used strong, tightly controlled promoters and strong ribosome binding sites for plasmids harboring the enzymes. In contrast to other metabolic engineering efforts, our approach does not require the focus on flux balancing and delicate promoter tuning to maintain viability as for *in vivo* systems.[4, 15–17] Our goal is to maximally express proteins *in vivo*, then mix-and-match corresponding lysates to optimize cell-free production (without viability[19, 20] and growth constraints of cells). As expected, we observed that the heterologous proteins were overexpressed as the dominant bands on an SDS-PAGE gel of the extracts (Figure S1).

After lysis and extract preparation, we reconstituted the pathway from glucose to mevalonate by mixing three separate extracts containing an overexpressed enzyme (ACAT, HMGS, or HMGR) with salts and substrates to initiate the cell-free biosynthesis reaction. The CFME

reaction contains extract, substrate (glucose), catalytic amounts of cofactors (1 mM NAD^+ and 1 mM CoA), 1 mM ATP, and acetate salts to mimic the cytoplasmic environment. In addition, free phosphate was supplemented (10 mM) in a manner consistent with previous work where cell-free protein synthesis was energized from glucose and G6P.[46] Cation concentrations (Mg^{2+}, NH_4^+, and K^+) were based on our previous work[33] and are consistent with principles of cytoplasmic mimicry.[44, 47] Initially, glutamate was used as the counter-ion for magnesium, potassium, and ammonium salts.[47] However, acetate salts were found to achieve higher mevalonate titers (Figure S2) and were subsequently used for the remainder of the study.

Our initial analysis used heterologous HMGS and HMGR sequences from *Saccharomyces cerevisiae*, as described by Dueber and coworkers.[43] Upon incubation with essential substrates, we assessed mevalonate synthesis in 25 μl CFME batch reactions carried out for 24 hours at 37 °C via gas chromatography mass spectroscopy (GC-MS). After 9 hours, 12.8 ± 1.3 mM of mevalonate (~1.6 g·L^{-1}) was generated at a linear productivity of 1.43 ± 0.15 g·L^{-1}·hr^{-1}. NAD(P)H and ATP are not limiting in this cell-free reaction since the extract contains enzymes that convert glucose to NAD(P)H and microsome vesicles that produce ATP from proton motive force.[44]

Evaluation of enzyme variants for mevalonate production

Following demonstration of active mevalonate synthesis with our CFME approach, we leveraged extract mixing to modularly identify best performing enzyme homologs (Table 1) as well as evaluate differences in cofactor specificity (NADH vs. NADPH). We first tested NADPH-preferring HMGRs from three different organisms: *S. cerevisiae, Enterococcus faecalis*, and *Staphylococcus aureus*. In 24-hour CFME reactions with 200 mM glucose (with or without 1mM $NADP^+$ supplementation), we observed mevalonate titers ranging from 3.7 to 70.9 mM (Figure 2A). The Type I HMGR from eukaryotic *S. cerevisiae* exclusively uses NADPH and produces the lowest mevalonate titer. However, it is a truncated enzyme containing only the catalytic domain, which may affect its stability and/or catalytic activity. Unique for a Type ll HMGR, the *E. faecalis* version is also NADPH-dependent[51] and is a bifunctional enzyme fused to ACAT. The *E. faecalis* HMGR increased mevalonate titer 3-fold over the yeast HMGR. Finally, we found the Type II HMGR from *S. aureus* to be the most active homolog, perhaps because it is able to utilize both NADH and NADPH despite NADPH being its preferred cofactor.[52] Validating our method for identifying active sets of enzymes through our mix-and-match approach, the HMGR from *S. aureus* has been previously identified as outperforming the variant from *S. cerevisiae*.[48]

In contrast to the abbreviated metabolic pathway depicted in Figure 1A, the activity of NADPH-dependent HMGRs (Figure 2A) demonstrates generation of NADPH by the cell-free system. Two sources of NADPH are most likely: First, oxidation of glucose through the pentose phosphate pathway generates NADPH catalyzed by glucose-6-phosphate dehydrogenase *(zwf)* and 6-phosphogluconate dehydrogenase *(gnd)*. Alternatively, soluble *(sthA)* or membrane-bound *(PntBA)* transhydrogenase enzymes present in the extract may be generating NADPH and NAD^+ from substrates NADH and $NADP^+$. In effort to provide

additional NADPH to the system, we added transhydrogenase (*sthA*)-enriched extract to the reaction, but did not observe an increase mevalonate titer (Figure S3).

To extend our analysis, we considered NADH-dependent Type II HMGRs. In our experiments, these enzymes generated the highest mevalonate titers (Figure 2B), particularly those from *Pseudomonas mevalonii* and *Bordetella petrii*. This is consistent with the expectation that Embden-Meyerhof-Parnas glycolysis described in Figure 1A generates NADH reducing equivalents which are directly available for reducing HMG-CoA to mevalonate. Compared to our base case (*S. cerevisiae* HMGR: 12.8 ± 1.3 mM over 9 hours), titers are ~6-fold higher for the *P. mevalonii* HMGR (84.2 ± 8.1 mM over 15 hours). Variation of the second enzyme (HMGS) increased the rate of synthesis slightly; however, the *S. cerevisiae* homolog gives the highest final titer (Figure 2B). The mixing-and-matching of lysates informed the selection of ACAT from *E. coli*, HMGS from *S. cerevisiae*, and HMGR from *P. mevalonii* for further characterization.

Testing of enzyme ratios and guided construction of an all-in-one source strain

A key conceptual shift of our approach is that the design element is a lysate rather than a gene. Once in hand, selectively enriched lysates can be mixed in different ratios to assemble new pathways, estimate beneficial enzyme proportions, and determine which enzymes might be rate-limiting (Figure 3A). In this work, extract ratios were calculated as a fraction of total protein mass (mg·mL^{-1}) in the CFME reaction (each reaction contained 10 mg·mL^{-1} total protein). Notably, each enzyme was overexpressed to similar levels in the lysate (Figure 3B). We observed that overall mevalonate yields from glucose were relatively insensitive to different extract ratios.

We next set out to construct an all-in-one extract from a source strain overexpressing all three pathway enzymes, as we had previously reported on for the production of 2,3-butanediol.[33] To do this, we needed to clone the entire pathway for mevalonate onto a single plasmid using design rules for enzyme sets and pathway ratios above. It is well known that genes positioned earlier in an operon have a higher relative expression level.[53] Since higher ratios of HMGR and HMGS may be better (Figure 3A), HMGR and HMGS were placed first on the plasmid, followed by ACAT (Table 1). After lysate preparation, SDS-PAGE confirmed that the single strain expresses all three proteins at similar levels to the individually mixed condition (Figure 3B).

We next compared mevalonate production between our all-in-one and mix-and-match systems in a 28 hour CFME reaction. The all-in-one extract system performs similarly to three extracts mixed at equal ratios (Figure 3C). We observed that pH decreases over the course of reaction in both systems, possibly due to an increased in dissolved carbon dioxide from pyruvate decarboxylation.[54] Upon testing a number of buffers, we found 100 mM and 200 mM Bis-Tris to successfully stabilize reaction pH closer to 7.0 and produce the same titer of mevalonate.

One important consideration in CFME is the desire to have the same amount of soluble heterologously expressed protein in the extract when comparing enzyme homologs. While most overexpressed enzymes have some portion that is insoluble (Figure S4A), extract

preparation removes insoluble proteins and cellular debris. Thus, solubility of a homolog does not obscure its apparent activity. However, apparent activity could be impacted by the percentage of soluble overexpressed enzyme in each extract (in our experiments this varied from ~ 4–24% of the total protein content of the extract; Figure S4A). Since altering the ratio of each extract has a small effect on overall mevalonate titer (Figure 3A), we suspect that overexpressed enzyme concentration is not limiting in our experiments. This conclusion is supported by our recent work in using lysates to synthesize 2,3-butanediol where heterologous pathway flux is limited by glycolysis.[33] While we find little to no correlation between mevalonate titer and recombinant protein expression level (Figure S4B), we acknowledge that enzyme overexpression is a potential source of variation that could be controlled for using a normalization step.[55] Another consideration for CFME is that proteins which express poorly may not be good candidates for this prototyping approach. Finally, we highlight that the toxicity pressure of some intermediates, such as HMG CoA,[19, 20] may not be accurately captured in the CFME prototyping strategy, representing a potential shortcoming.

Optimization of cofactors

An important consideration in cell-free systems is the concentrations of salts and cofactors. Indeed, it has been shown that ionic compositions and reaction conditions that closely reflect the cytoplasm are beneficial for activating multiple metabolic and energy regeneration pathways.[44, 47, 56, 57] To provide an example of CFME's prototyping capabilities, we studied the impact of initial cofactor ratios on mevalonate synthesis. CFME reactions were carried out for 24 hours in which the supplemental cofactors NAD^+, ATP, and CoA were removed one-by-one, in pairs, and altogether (Figure 4A). This revealed NAD^+ to be critical to high mevalonate titer; its absence reduced mevalonate concentration by over half. Relatively high mevalonate titers were maintained without supplementation of ATP (required for the pay-in phase of glycolysis) and CoA (a cofactor for the pyruvate dehydrogenase complex converting pyruvate to acetyl-CoA).

Surprisingly, glucose, acetate salts, phosphate, and extract can support ~80% of yield without any supplementary cofactors (Figure 4A: red bar). These results suggest that intracellular cofactors (such as NAD^+, ATP, and CoA) are carried over from the cytoplasm into the extract during extract preparation and are at sufficient concentration to drive mevalonate synthesis. To verify this hypothesis, we directly measured the NAD^+ concentration in the cell-free reaction without supplementation. We found the NAD^+ concentration to be 0.09 ± 0.035 mM (Figure S5). Each conversion of HMG-CoA to mevalonate requires two reducing equivalents, thus, the system with 1mM NAD^+ supplementation has ~200 turnover events while the system without supplementation has ~1250. These values are two orders of magnitude higher than typical turnover values of purified CFME systems (5–20 turnover events),[22] and are similar to those of state-of-the-art crude extract systems.[32, 33] While the main goal of our study was to develop a new CFME framework for modularly prototyping enzyme homologs and reaction conditions, the possibility of achieving high titers without costly cofactor supplementation is important if one envisions using CFME for industrial applications.

Direct access to the cell-free reaction increases the resolution at which biochemical conditions can be manipulated compared to living systems. We therefore sought to further explore concentration-dependent effects of NAD^+, ATP, and CoA in the CFME reaction. Specifically, we modulated concentrations from 0 to 1 to 10 mM for NAD^+ and ATP at two different CoA concentrations (0 and 1 mM) (Figure 4B and 4C). The two landscapes offer different trends with no obvious shared pattern, indicating a complex interplay between cofactor concentrations, extract components and resulting metabolic fluxes. Interestingly, our initial choice of concentrations (1 mM each) proved to generate a nearly equivalent mevalonate titer compared to the best condition (Figure 4C).

Source strain genome engineering to redirect metabolic flux: knockout of ldhA, acs, and ackA-pta

Knockout of competing metabolic pathways is a common strategy in metabolic engineering to increase product titer.[13] As crude lysates contain many other endogenous enzymes in addition to our desired pathway enzymes (Figure 5A), it is possible that competing pathways siphon carbon flux from mevalonate biosynthesis (Figure 5B). We therefore next studied our CFME reactions by monitoring small molecule organic acid concentrations at selected time points in batch reactions using high performance liquid chromatography (HPLC). Quantification revealed that lactate (Figure 5C), and pyruvate (Figure 5D) accumulate while glucose (Figure 5E) and acetate (Figure 5F) concentrations decrease over the course of the reaction. Phosphate, ethanol, oxaloacetate concentrations remained constant (Figure S6).

To elucidate the role of lactate and acetate metabolism, knockout mutations were made in the source strain prior to extract preparation using the Datsenko-Wanner technique[58] (Figure 5A). The idea of modifying extract source strains is not new in cell-free synthetic biology and has been used for enhancing cell-free protein synthesis systems,[59, 60] however, source strain gene knockouts have been underutilized in the cell-free metabolic engineering context with only one other known example to date.[31]

To prevent lactate accumulation, we deleted the *ldhA* gene (encoding lactate dehydrogenase) in the extract source strain. The knockout was confirmed by PCR (Figure S7) and by sequencing (see Appendix S2). After generating extract with mevalonate pathway genes, we carried out a 24 hour CFME reaction. Mevalonate synthesis rates and titers were halved as compared to the control (extract containing *ldhA*). Glucose and acetate consumption rates are consistent with wild type for the first 6 hours; after this, however, the consumption rates slow. We hypothesize that the decrease in mevalonate titer is because lactate dehydrogenase is no longer available to recycle excess NADH to NAD+. This cofactor recycle is necessary because the enzymatic pathway is not cofactor balanced (Figure 1C). Without lactate dehydrogenase, a low amount of succinate accumulates as the TCA cycle fixes acetyl-CoA and consumes NADH to make succinate (Figure S6). Although lactate accumulation diverts carbon flow from mevalonate, it appears that non-lactate sinks for excess NADH are saturated after six hours, ultimately limiting mevalonate titer.

To understand the impact of acetate metabolism on mevalonate synthesis, we made a series of mutant extract source strains. Acetate catabolism in *E. coli* occurs via the *acs* enzyme or the *ackA-pta* pathway, both of which require ATP (Figure 5A). Unlike the wild type system,

the concentration of acetate in *ΔackA-pta* and *ΔacsΔackA-pta* extracts remained constant at 200 mM (Figure 5F); this indicates that acetate kinase (*ackA*) and phosphate acetyltransferase (*pta*) were active in the wild type scenario. Without these enzymes, mevalonate synthesis was reduced to ~5 mM and much less glucose was consumed (70 mM) compared to the wild type system (180 mM). In contrast, the acetyl-CoA synthase knockout (*Δacs*) performed identical to wild type. These results suggest that *ackA* and *pta* are converting acetate to acetyl-CoA, which is subsequently available as a substrate for incorporation into mevalonate (Figure 5A). This may explain the improvement in mevalonate titers when using acetate salts compared to glutamate or chloride salts (Figure S2). Since knockout of *ackA* and *pta* are deleterious to mevalonate titers, we hypothesize that these enzymes may be important in converting excess ATP from glycolysis to ADP; however, further experimentation would be needed to assess this.

Evaluation of freeze-dried extracts for distributed biomanufacturing

High-level cofactor regeneration is an important first step for prospective cell-free biomanufacturing applications using crude extracts.[22] With this result at hand, we evaluated the potential to freeze-dry the complete CFME system and maintain high biosynthesis activity for distributed manufacturing applications. Recently, Bundy and colleagues used lyophilized extracts to make the therapeutic protein onconase[61] as well as other proteins. [62, 63] Additionally, Collins and coworkers have pioneered paper-based, colorimetric diagnostics using toehold switches and freeze dried lysates to detect Ebola[64] and Zika[65] viral RNA. These studies indicate that the components required for cell-free biosynthesis are active after lyophilization and point to freeze drying as a useful means of storing lysates for therapeutic and diagnostic applications. Here, we freeze-dried the complete CFME system containing the lysate with selectively enriched pathway enzymes, substrates and salts. By rehydrating the system, we observed similar mevalonate synthesis rates and titers when compared to the non-freeze dried system (Figure 6). This supports a possible vision of on-demand, "just-add-water cell-free systems".[61]

Summary

To our knowledge, this work is the first demonstration of mixing multiple selectively enriched crude extracts to reconstitute a metabolic pathway. Specifically, we showed the ability to reconstitute the pathway from glucose to mevalonate by mixing three enzyme-enriched lysates. We improved mevalonate titer at 15 hours from our initial case of 1.6 g·L^{-1} (12.8 mM) to 12.5 g·L^{-1} (84.2 mM) by prototyping enzyme homologs (Figure 2B/C). After developing an all-in-one source strain with optimization of small molecule cofactors, the titer increased to 17.6 g·L^{-1} (119 mM) over 20 hours; this titer correlates to a productivity of 0.88 g·L^{-1}·hr^{-1} (Figure 4C). Using the *ackA-pta* pathway to metabolize acetate as a carbon source in addition to glucose (Figure 5), the overall carbon yield is 0.35 mol carbon product / mol carbon substrate (when accounting for CO_2 lost, the stoichiometric maximum is 0.75 mol product / mol substrate) (Appendix S3). This is 46.9% of theoretical yield. Turnover of the cofactor NAD$^+$ was ~1250 when not supplemented. This value is higher than most purified enzyme systems[22] and similar to two other recent publications.[32, 33] The ability of crude extract native metabolism to recycle excess ATP and NADH highlights a potential advantage of lysate-based CFME. Of note, our work complements efforts by

several groups to prototype isoprenoid synthesis using purified enzymes,[37, 66–68] as well as *in vivo* metabolic engineering efforts (Table S1),[43, 69–71]

Within cell-free synthetic systems, there is growing interest to prototype pathway performance,[34–42] such as a recent report that demonstrates mixing of purified enzymes with a crude extract in a glucose-to-hydrogen enzyme pathway[72] and another exploring fatty acid biosynthesis.[34] As a prototyping platform, testing of new enzyme variants by CFME requires only purchasing the gene, one-step cloning into an expression vector, preparing extract, and running a cell-free reaction. In a parallel effort, we extended the concept here to include cell-free protein synthesis, where lysates are selectively enriched, not by heterologous expression, but by producing the pathway enzymes directly from linear PCR templates in cell-free protein synthesis reactions.[73] This approach accelerates the timeline of prototyping and could be leveraged to express and evaluate membrane proteins.[74]

In summary, our work demonstrates the high activity of CFME extracts and outlines an extract mixing approach allows easy screening of enzyme variants. Looking forward, we expect that our approach will complement existing strategies for gene discovery and pathway prototyping by changing the focus of the biosynthesis "unit operation" from the cell to the lysate, enabling the use of multiple organisms with or without additional genetic engineering.

Materials and methods

Strains and plasmids

All strains and plasmids for this study are listed in Table 1. Mevalonate pathway genes from *E. coli* (ACAT) and *S. cerevisiae* (HMGS/HMGR) were obtained from pGW322,[43] kindly provided by Jay Keasling. Sequences were PCR-amplified using Phusion polymerase and primers which contained appropriate EcoRI, BglII, BamHI, and XhoI restriction sites used by the Berkeley Cloning Standard (BCS).[75] The remaining HMGS and HMGR amino acid sequences were obtained from the Universal Protein Resource (UniProt), codon optimized for expression in *E. coli*, and synthesized (with flanking BCS restriction sites) by Gen9 (Cambridge, MA) or Integrated DNA Technologies (Coralville, IA). Ribosome binding site (RBS) sequences were designed and optimized to be greater than 30,000 arbitrary units using the Salis RBS calculator (v1.1).[76] Sequences are available in the supplement (Appendix S1).

Gene sequences were digested and ligated into pETBCS, a modified pET-22b vector (Novagen/EMD Millipore, Darmstadt, Germany) with signal sequence removed and modified restriction sites.[33] Routine cloning was performed using the *E. coli* strain NEB Turbo™ and all DNA-modifying enzymes were purchased from NEB (New England BioLabs, Ipswich, MA).

BL21(DE3) (purchased from Invitrogen / Thermo Fisher Scientific, Waltham, MA) was used as the source strain for extract production. Knockout strains were generated using the Datsenko-Wanner technique,[58] where the complete gene coding sequence (from start to stop

codon) was replaced by a non-coding "scar" sequence containing the FRT recognition sequence. Sequences are available in the supplement (Appendix S2).

Cell growth and extract preparation

E. coli containing the appropriate pETBCS-based plasmid (harboring one or more pathway genes) were grown in 1-liter Tunair™ shake flasks at 37 °C (250 rpm) in rich media (18 g·L^{-1} glucose, 16 g·L^{-1} yeast extract, 10 g·L^{-1} tryptone, 5 g·L^{-1} NaCl, 7 g·L^{-1} potassium phosphate dibasic (K_2HPO_4), 3 g·L^{-1} potassium phosphate monobasic (KH_2PO_4)) containing 100 μg·mL^{-1} carbenicillin (IBI Scientific, Peosta, IA). BD Bacto™ brand media components tryptone and yeast extract were obtained from BD Biosciences (San Jose, CA). Cultures were induced with 0.1mM IPTG (Santa Cruz Biotech, Dallas, TX) at 0.6 OD_{600nm} and growth continued at 30 °C until harvest. Four hours post-induction, cultures were harvested following previously established protocols.[33, 44] Cells were pelleted by centrifugation (8000 × *g* for 15 minutes) and the resulting pellet was rinsed twice in S30 buffer (10 mM tris acetate pH 8.2, 14 mM magnesium acetate, and 60 mM potassium acetate), and flash-frozen for storage at −80 °C.

To generate crude extracts, cell pellets were thawed on ice and suspended in S30 buffer (0.8 mL per gram cell pellet), and lysed at 20,000 psi (homogenizing pressure) using an EmulsiFlex-B15 homogenizer (Avestin, Ottawa, ON). While all results reported here use high pressure homogenization, cells grown at small scale (50 mL) and lysed by sonication following established protocols[77] performed similarly (data not shown). Total protein was quantified by Bradford assay with bovine serum albumin (BSA) as the standard using a microplate protocol (Bio-Rad, Hercules, CA). Overexpression of enzymes was confirmed by NuPAGE® SDS-PAGE protein gels using Coomassie stain (Life Technologies / Thermo Fisher Scientific, Waltham, MA).

Cell free biosynthesis of mevalonate

Cell free reactions were performed at a volume of 25 μL in 1.5 mL Eppendorf tubes and incubated at 37 °C. The standard reaction contained the following components: 200 mM glucose, acetate salts (8mM magnesium acetate, 10mM ammonium acetate, 134 mM potassium acetate), and 10mM potassium phosphate (K_2HPO_4, pH 7.2).[46] Unless specified, reactions also included 1mM NAD$^+$, 1mM ATP, and 1mM CoA.[33] All reagents and chemicals were purchased from Sigma Aldrich (St. Louis, MO).

Extract concentration for all CFME reactions was 10 mg·mL^{-1} total protein. When mixing lysates, the relative levels of each were adjusted to maintain a total protein concentration of 10 mg·mL^{-1}. Reactions were quenched by precipitating proteins using 25 μL of 5% trichloroacetic acid (TCA) and then centrifuging at 15,000 × *g* for 10 minutes at 4 °C. The supernatant was collected and stored at −80 °C until analysis by GC-MS or HPLC.

Lyophilization of CFME reactions

Cell-free reactions were assembled as described above. Upon mixing, reactions were immediately flash frozen in liquid nitrogen. Lyophilization took place in 25 μL volumes using a VirTis BenchTop Pro lyophilizer (SP Scientific, Warminster, PA) set to −86 °C and

<500 mTorr for 16.5 hours. To reinitiate the CFME reaction, 25 μL of water was added to rehydrate the pellet.

Quantification of mevalonate, NAD⁺, and organic acids.

Mevalonate was quantified using an Agilent 7890A Gas Chromatograph with 5977A MSD (Agilent, Santa Clara, CA) based on a method adapted from Dueber *et al.*[43, 78] 10 μL of precipitated reaction supernatant was additionally acidified by 5 μL of 0.5M HCl to convert mevalonate to mevalonolactone via acid-catalyzed esterification. Samples were then extracted via mixing with 210 μL ethyl acetate spiked with 50 μg/mL trans-caryophyllene (Sigma), vortexed for 3 min, then centrifuged for at $2000 \times g$ for 3 min using 4445.x microcentrifuge tubes (Neptune Scientific, San Diego, CA). The ethyl acetate fraction was then run on an Agilent HP-5MS (30 m length × 0.25mm i.d. × 0.25 μm film) column with helium carrier gas at constant flow of 1 mL·min^{-1}. The inlet temperature was 150 °C and column temperature started at 150 °C, increased at 30 °C/min to 240 °C, and was held at 240 °C for 0.5 minutes. Injection volume is 1 μL with a split ratio of 75:1. Extract ion chromatograms (EIC) for 71.0 m/z and 133.1 m/z were integrated using Agilent MassHunter Quantitation Analysis software. Concentration was determined by comparison to standards prepared by mixing dilutions of (±)-mevalonolactone (Sigma) with 152 mM acetate salts, 10 mM K_2HPO_4, and 10 mg·mL^{-1} of BL21 extract (which contains no expressed proteins with catalytic activity to mevalonate). Standards were quenched with 5% TCA and prepared as described above.

NAD⁺ and NADH were quantified using a fluorescent kit (Sigma). Cell free reactions were quenched by diluting 1:200 in the kit extraction buffer and immediately freezing in liquid nitrogen. Samples were then thawed and prepared following the kit protocol.

Glucose, acetate, lactate, pyruvate, succinate, oxaloacetate, phosphate, and ethanol were measured via refractive index (RI) using an Agilent 1260 HPLC system (Agilent, Santa Clara, CA). Precipitated sample supernatant was separated isocratically on an Aminex HPX-87H column (Bio-Rad, Hercules, CA) heated to 55 °C with a mobile phase of 5 mM H_2SO_4 and flow rate of 0.6 mL·min^{-1}. Concentration was determined by comparison to standards of known concentration.

Supplementary Material

Refer to Web version on PubMed Central for supplementary material.

Acknowledgements

References

[1]. Bohlmann J, and Keeling CI (2008) Terpenoid biomaterials, The Plant Journal 54, 656–669. [PubMed: 18476870]

[2]. Leavell MD, McPhee DJ, and Paddon CJ (2016) Developing fermentative terpenoid production for commercial usage, Current opinion in biotechnology 37, 114–119. [PubMed: 26723008]

[3]. Paddon CJ, Westfall PJ, Pitera DJ, Benjamin K, Fisher K, McPhee D, Leavell MD, Tai A, Main A, Eng D, Polichuk DR, Teoh KH, Reed DW, Treynor T, Lenihan J, Fleck M, Bajad S, Dang G, Dengrove D, Diola D, Dorin G, Ellens KW, Fickes S, Galazzo J, Gaucher SP, Geistlinger T, Henry R, Hepp M, Horning T, Iqbal T, Jiang H, Kizer L, Lieu B, Melis D, Moss N, Regentin R, Secrest S, Tsuruta H, Vazquez R, Westblade LF, Xu L, Yu M, Zhang Y, Zhao L, Lievense J, Covello PS, Keasling JD, Reiling KK, Renninger NS, and Newman JD (2013) High-level semi-synthetic production of the potent antimalarial artemisinin, Nature 496, 528–532. [PubMed: 23575629]

[4]. Ajikumar PK, Xiao W-H, Tyo KE, Wang Y, Simeon F, Leonard E, Mucha O, Phon TH, Pfeifer B, and Stephanopoulos G (2010) Isoprenoid pathway optimization for Taxol precursor overproduction in Escherichia coli, Science 330, 70–74. [PubMed: 20929806]

[5]. Zurbriggen A, Kirst H, and Melis A (2012) Isoprene production via the mevalonic acid pathway in Escherichia coli (Bacteria), BioEnergy Research 5, 814–828.

[6]. Leonard E, Ajikumar PK, Thayer K, Xiao W-H, Mo JD, Tidor B, Stephanopoulos G, and Prather KL (2010) Combining metabolic and protein engineering of a terpenoid biosynthetic pathway for overproduction and selectivity control, Proceedings of the National Academy of Sciences 107, 13654–13659.

[7]. Alonso-Gutierrez J, Chan R, Batth TS, Adams PD, Keasling JD, Petzold CJ, and Lee TS (2013) Metabolic engineering of Escherichia coli for limonene and perillyl alcohol production, Metabolic engineering 19, 33–41. [PubMed: 23727191]

[8]. George KW, Thompson MG, Kang A, Baidoo E, Wang G, Chan LJG, Adams PD, Petzold CJ, Keasling JD, and Lee TS (2015) Metabolic engineering for the high-yield production of isoprenoid-based C5 alcohols in E. coli, Scientific reports 5.

[9]. George KW, Alonso-Gutierrez J, Keasling JD, and Lee TS (2015) Isoprenoid Drugs, Biofuels, and Chemicals—Artemisinin, Farnesene, and Beyond, Advances in biochemical engineering/biotechnology 148, 355–389. [PubMed: 25577395]

[10]. Li Y, and Pfeifer BA (2014) Heterologous production of plant-derived isoprenoid products in microbes and the application of metabolic engineering and synthetic biology, Current opinion in plant biology 19, 8–13. [PubMed: 24631884]

[11]. Nielsen J, Fussenegger M, Keasling J, Lee SY, Liao JC, Prather K, and Palsson B (2014) Engineering synergy in biotechnology, Nature Chemical Biology 10, 319–322. [PubMed: 24743245]

[12]. Keasling JD (2012) Synthetic biology and the development of tools for metabolic engineering, Metabolic engineering 14, 189–195. [PubMed: 22314049]

[13]. Lee JW, Na D, Park JM, Lee J, Choi S, and Lee SY (2012) Systems metabolic engineering of microorganisms for natural and non-natural chemicals, Nature Chemical Biology 8, 536–546. [PubMed: 22596205]

[14]. Nielsen J, and Keasling JD (2016) Engineering Cellular Metabolism, Cell 164, 1185–1197. [PubMed: 26967285]

[15]. Blazeck J, Liu L, Redden H, and Alper H (2011) Tuning gene expression in Yarrowia lipolytica by a hybrid promoter approach, Applied and environmental microbiology 77, 7905–7914. [PubMed: 21926196]

[16]. Du J, Yuan Y, Si T, Lian J, and Zhao H (2012) Customized optimization of metabolic pathways by combinatorial transcriptional engineering, Nucleic acids research 40, e142–e142. [PubMed: 22718979]

[17]. Biggs BW, De Paepe B, Santos CNS, De Mey M, and Ajikumar PK (2014) Multivariate modular metabolic engineering for pathway and strain optimization, Current opinion in biotechnology 29, 156–162. [PubMed: 24927371]

[18]. Nicolaou SA, Gaida SM, and Papoutsakis ET (2010) A comparative view of metabolite and substrate stress and tolerance in microbial bioprocessing: from biofuels and chemicals, to biocatalysis and bioremediation, Metabolic engineering 12, 307–331. [PubMed: 20346409]

[19]. Pitera DJ, Paddon CJ, Newman JD, and Keasling JD (2007) Balancing a heterologous mevalonate pathway for improved isoprenoid production in Escherichia coli, Metabolic engineering 9, 193–207. [PubMed: 17239639]

[20]. Kizer L, Pitera DJ, Pfleger BF, and Keasling JD (2008) Application of functional genomics to pathway optimization for increased isoprenoid production, Applied and environmental microbiology 74, 3229–3241. [PubMed: 18344344]

[21]. Hodgman CE, and Jewett MC (2012) Cell-free synthetic biology: thinking outside the cell, Metabolic engineering 14, 261–269. [PubMed: 21946161]

[22]. Dudley QM, Karim AS, and Jewett MC (2015) Cell-free metabolic engineering: Biomanufacturing beyond the cell, Biotechnology journal 10, 69–82. [PubMed: 25319678]

[23]. Rollin JA, Tam TK, and Zhang Y-HP (2013) New biotechnology paradigm: cell-free biosystems for biomanufacturing, Green Chemistry 15, 1708–1719.

[24]. Guterl JK, and Sieber V (2013) Biosynthesis "debugged": novel bioproduction strategies, Engineering in Life Sciences 13, 4–18.

[25]. Billerbeck S, Härle J, and Panke S (2013) The good of two worlds: increasing complexity in cell-free systems, Current opinion in biotechnology 24, 1037–1043. [PubMed: 23541502]

[26]. Swartz JR (2012) Transforming biochemical engineering with cell-free biology, AIChE Journal 58, 5–13.

[27]. Ye X, Honda K, Sakai T, Okano K, Omasa T, Hirota R, Kuroda A, and Ohtake H (2012) Synthetic metabolic engineering-a novel, simple technology for designing a chimeric metabolic pathway, Microbial cell factories 11, 120. [PubMed: 22950411]

[28]. Zhang Y-HP, Evans BR, Mielenz JR, Hopkins RC, and Adams MW (2007) High-yield hydrogen production from starch and water by a synthetic enzymatic pathway, PLoS One 2, e456. [PubMed: 17520015]

[29]. Guterl JK, Garbe D, Carsten J, Steffler F, Sommer B, Reiße S, Philipp A, Haack M, Rühmann B, Koltermann A, Kettling U, Bruck T, and Sieber V (2012) Cell-Free Metabolic Engineering: Production of Chemicals by Minimized Reaction Cascades, ChemSusChem 5, 2165–2172. [PubMed: 23086730]

[30]. Opgenorth PH, Korman TP, and Bowie JU (2016) A synthetic biochemistry module for production of bio-based chemicals from glucose, Nature chemical biology 12, 393–395. [PubMed: 27065234]

[31]. Bujara M, Schümperli M, Billerbeck S, Heinemann M, and Panke S (2010) Exploiting cell-free systems: Implementation and debugging of a system of biotransformations, Biotechnology and bioengineering 106, 376–389. [PubMed: 20091765]

[32]. Khattak WA, Ul-Islam M, Ullah MW, Yu B, Khan S, and Park JK (2014) Yeast cell-free enzyme system for bio-ethanol production at elevated temperatures, Process Biochemistry.

[33]. Kay JE, and Jewett MC (2015) Lysate of engineered *Escherichia coli* supports high-level conversion of glucose to 2, 3-butanediol, Metabolic engineering 32, 133–142. [PubMed: 26428449]

[34]. Liu T, Vora H, and Khosla C (2010) Quantitative analysis and engineering of fatty acid biosynthesis in E. coli, Metabolic engineering 12, 378–386. [PubMed: 20184964]

[35]. Wu YY, Culler S, Khandurina J, Van Dien S, and Murray RM (2015) Prototyping 1, 4-butanediol (BDO) biosynthesis pathway in a cell-free transcription-translation (TX-TL) system.

[36]. Bogorad IW, Lin T-S, and Liao JC (2013) Synthetic non-oxidative glycolysis enables complete carbon conservation, Nature 502, 693–697. [PubMed: 24077099]

[37]. Zhu F, Zhong X, Hu M, Lu L, Deng Z, and Liu T (2014) In vitro reconstitution of mevalonate pathway and targeted engineering of farnesene overproduction in Escherichia coli, Biotechnology and bioengineering 111, 1396–1405. [PubMed: 24473754]

[38]. Zhang Y, Meng Q, Ma H, Liu Y, Cao G, Zhang X, Zheng P, Sun J, Zhang D, and Jiang W (2015) Determination of key enzymes for threonine synthesis through in vitro metabolic pathway analysis, Microb Cell Fact 14, 86. [PubMed: 26070803]

[39]. Tan G-Y, Zhu F, Deng Z, and Liu T (2016) In vitro reconstitution guide for targeted synthetic metabolism of chemicals, nutraceuticals and drug precursors, Synthetic and Systems Biotechnology 1, 25–33. [PubMed: 29062924]

[40]. Siegal-Gaskins D, Tuza ZA, Kim J, Noireaux V, and Murray RM (2014) Gene Circuit Performance Characterization and Resource Usage in a Cell-Free "Breadboard", ACS Synthetic Biology.

[41]. Takahashi MK, Chappell J, Hayes CA, Sun ZZ, Kim J, Singhal V, Spring KJ, Al-Khabouri S, Fall CP, and Noireaux V (2014) Rapidly Characterizing the Fast Dynamics of RNA Genetic Circuitry with Cell-Free Transcription–Translation (TX-TL) Systems, ACS synthetic biology 4, 503–515. [PubMed: 24621257]

[42]. Karig DK, Iyer S, Simpson ML, and Doktycz MJ (2012) Expression optimization and synthetic gene networks in cell-free systems, Nucleic acids research 40, 3763–3774. [PubMed: 22180537]

[43]. Dueber JE, Wu GC, Malmirchegini GR, Moon TS, Petzold CJ, Ullal AV, Prather KL, and Keasling JD (2009) Synthetic protein scaffolds provide modular control over metabolic flux, Nature biotechnology 27, 753–759.

[44]. Jewett MC, Calhoun KA, Voloshin A, Wuu JJ, and Swartz JR (2008) An integrated cell-free metabolic platform for protein production and synthetic biology, Molecular systems biology 4, 220. [PubMed: 18854819]

[45]. Miziorko HM (2011) Enzymes of the mevalonate pathway of isoprenoid biosynthesis, Archives of biochemistry and biophysics 505, 131–143. [PubMed: 20932952]

[46]. Calhoun KA, and Swartz JR (2005) Energizing cell-free protein synthesis with glucose metabolism, Biotechnology and bioengineering 90, 606–613. [PubMed: 15830344]

[47]. Jewett MC, and Swartz JR (2004) Mimicking the Escherichia coli cytoplasmic environment activates long-lived and efficient cell-free protein synthesis, Biotechnology and bioengineering 86, 19–26. [PubMed: 15007837]

[48]. Tsuruta H, Paddon CJ, Eng D, Lenihan JR, Horning T, Anthony LC, Regentin R, Keasling JD, Renninger NS, and Newman JD (2009) High-level production of amorpha-4, 11-diene, a precursor of the antimalarial agent artemisinin, in Escherichia coli, PloS one 4, e4489. [PubMed: 19221601]

[49]. Ma SM, Garcia DE, Redding-Johanson AM, Friedland GD, Chan R, Batth TS, Haliburton JR, Chivian D, Keasling JD, Petzold CJ, Lee TS, and Chhabra SR (2011) Optimization of a heterologous mevalonate pathway through the use of variant HMG-CoA reductases, Metabolic engineering 13, 588–597. [PubMed: 21810477]

[50]. Yoon S-H, Lee S-H, Das A, Ryu H-K, Jang H-J, Kim J-Y, Oh D-K, Keasling JD, and Kim S-W (2009) Combinatorial expression of bacterial whole mevalonate pathway for the production of β-carotene in E. coli, Journal of biotechnology 140, 218–226. [PubMed: 19428716]

[51]. Hedl M, Sutherlin A, Wilding EI, Mazzulla M, McDevitt D, Lane P, Burgner JW, Lehnbeuter KR, Stauffacher CV, and Gwynn MN (2002) Enterococcus faecalis acetoacetyl-coenzyme A thiolase/3-hydroxy-3-methylglutaryl-coenzyme A reductase, a dual-function protein of isopentenyl diphosphate biosynthesis, Journal of bacteriology 184, 2116–2122. [PubMed: 11914342]

[52]. Wilding EI, Kim D-Y, Bryant AP, Gwynn MN, Lunsford RD, McDevitt D, Myers JE, Rosenberg M, Sylvester D, and Stauffacher CV (2000) Essentiality, Expression, and Characterization of the Class II 3-Hydroxy-3-Methylglutaryl Coenzyme A Reductase ofStaphylococcus aureus, Journal of bacteriology 182, 5147–5152. [PubMed: 10960099]

[53]. Lim HN, Lee Y, and Hussein R (2011) Fundamental relationship between operon organization and gene expression, Proceedings of the National Academy of Sciences 108, 10626–10631.

[54]. Welch P, and Scopes RK (1985) Studies on cell-free metabolism: Ethanol production by a yeast glycolytic system reconstituted from purified enzymes, Journal of biotechnology 2, 257–273.

[55]. Batth TS, Singh P, Ramakrishnan VR, Sousa MM, Chan LJG, Tran HM, Luning EG, Pan EH, Vuu KM, and Keasling JD (2014) A targeted proteomics toolkit for high-throughput absolute quantification of Escherichia coli proteins, Metabolic engineering 26, 48–56. [PubMed: 25205128]

[56]. Record MT, Courtenay ES, Cayley S, and Guttman HJ (1998) Biophysical compensation mechanisms buffering E. coli protein–nucleic acid interactions against changing environments, Trends in Biochemical Sciences 23, 190–194. [PubMed: 9612084]

[57]. Jewett MC, Fritz BR, Timmerman LE, and Church GM (2013) In vitro integration of ribosomal RNA synthesis, ribosome assembly, and translation, Mol Syst Biol 9, 678. [PubMed: 23799452]

[58]. Datsenko KA, and Wanner BL (2000) One-step inactivation of chromosomal genes in Escherichia coli K-12 using PCR products, Proceedings of the National Academy of Sciences 97, 6640–6645.

[59]. Hong SH, Kwon YC, Martin RW, Des Soye BJ, de Paz AM, Swonger KN, Ntai I, Kelleher NL, and Jewett MC (2015) Improving Cell-Free Protein Synthesis through Genome Engineering of Escherichia coli Lacking Release Factor 1, ChemBioChem 16, 844–853. [PubMed: 25737329]

[60]. Schoborg JA, Clark LG, Choudhury A, Hodgman CE, and Jewett MC (2016) Yeast knockout library allows for efficient testing of genomic mutations for cell-free protein synthesis, Synthetic and Systems Biotechnology 1, 2–6. [PubMed: 29062921]

[61]. Salehi AS, Smith MT, Bennett AM, Williams JB, Pitt WG, and Bundy BC (2016) Cell-free protein synthesis of a cytotoxic cancer therapeutic: Onconase production and a just-add-water cell-free system, Biotechnology journal 11, 274–281. [PubMed: 26380966]

[62]. Smith MT, Berkheimer SD, Werner CJ, and Bundy BC (2014) Lyophilized Escherichia coli-based cell-free systems for robust, high-density, long-term storage, BioTechniques 56, 186–193. [PubMed: 24724844]

[63]. Smith MT, Bennett AM, Hunt JM, and Bundy BC (2015) Creating a completely "cell-free" system for protein synthesis, Biotechnology progress 31, 1716–1719. [PubMed: 26289032]

[64]. Pardee K, Green AA, Ferrante T, Cameron DE, DaleyKeyser A, Yin P, and Collins JJ (2014) Paper-based synthetic gene networks, Cell 159, 940–954. [PubMed: 25417167]

[65]. Pardee K, Green AA, Takahashi MK, Braff D, Lambert G, Lee JW, Ferrante T, Ma D, Donghia N, and Fan M (2016) Rapid, low-cost detection of Zika virus using programmable biomolecular components, Cell 165, 1255–1266. [PubMed: 27160350]

[66]. Chen X, Zhang C, Zou R, Zhou K, Stephanopoulos G, and Too HP (2013) Statistical Experimental Design Guided Optimization of a One-Pot Biphasic Multienzyme Total Synthesis of Amorpha-4, 11-diene, PloS one 8, e79650. [PubMed: 24278153]

[67]. Korman TP, Sahachartsiri B, Li D, Vinokur JM, Eisenberg D, and Bowie JU (2014) A synthetic biochemistry system for the in vitro production of isoprene from glycolysis intermediates, Protein Science.

[68]. Rodriguez SB, and Leyh TS (2014) An enzymatic platform for the synthesis of isoprenoid precursors.

[69]. Tabata K, and Hashimoto S-I (2004) Production of mevalonate by a metabolically-engineered Escherichia coli, Biotechnology letters 26, 1487–1491. [PubMed: 15604784]

[70]. Xiong M, Schneiderman DK, Bates FS, Hillmyer MA, and Zhang K (2014) Scalable production of mechanically tunable block polymers from sugar, Proceedings of the National Academy of Sciences 111, 8357–8362.

[71]. Rodriguez S, Denby CM, Vu T. v., Baidoo EE, Wang G, and Keasling JD (2016) ATP citrate lyase mediated cytosolic acetyl-CoA biosynthesis increases mevalonate production in Saccharomyces cerevisiae, Microbial cell factories 15, 1. [PubMed: 26729212]

[72]. Lu F, Smith PR, Mehta K, and Swartz JR (2015) Development of a synthetic pathway to convert glucose to hydrogen using cell free extracts, International Journal of Hydrogen Energy 40, 9113–9124.

[73]. Karim AS, and Jewett MC (2016) A cell-free framework for rapid biosynthetic pathway prototyping and enzyme discovery, Metabolic Engineering 36, 116–126. [PubMed: 26996382]

[74]. Sachse R, Dondapati SK, Fenz SF, Schmidt T, and Kubick S (2014) Membrane protein synthesis in cell-free systems: From bio-mimetic systems to bio-membranes, FEBS letters 588, 2774–2781. [PubMed: 24931371]

[75]. Anderson JC, Dueber JE, Leguia M, Wu GC, Goler JA, Arkin AP, and Keasling JD (2010) BglBricks: A flexible standard for biological part assembly, Journal of biological engineering 4, 1–12. [PubMed: 20205762]

[76]. Salis HM, Mirsky EA, and Voigt CA (2009) Automated design of synthetic ribosome binding sites to control protein expression, Nature biotechnology 27, 946–950.

[77]. Kwon Y-C, and Jewett MC (2015) High-throughput preparation methods of crude extract for robust cell-free protein synthesis, Scientific reports 5.

[78]. Rodriguez S, Kirby J, Denby CM, and Keasling JD (2014) Production and quantification of sesquiterpenes in Saccharomyces cerevisiae, including extraction, detection and quantification of terpene products and key related metabolites, Nature protocols 9, 1980–1996. [PubMed: 25058645]
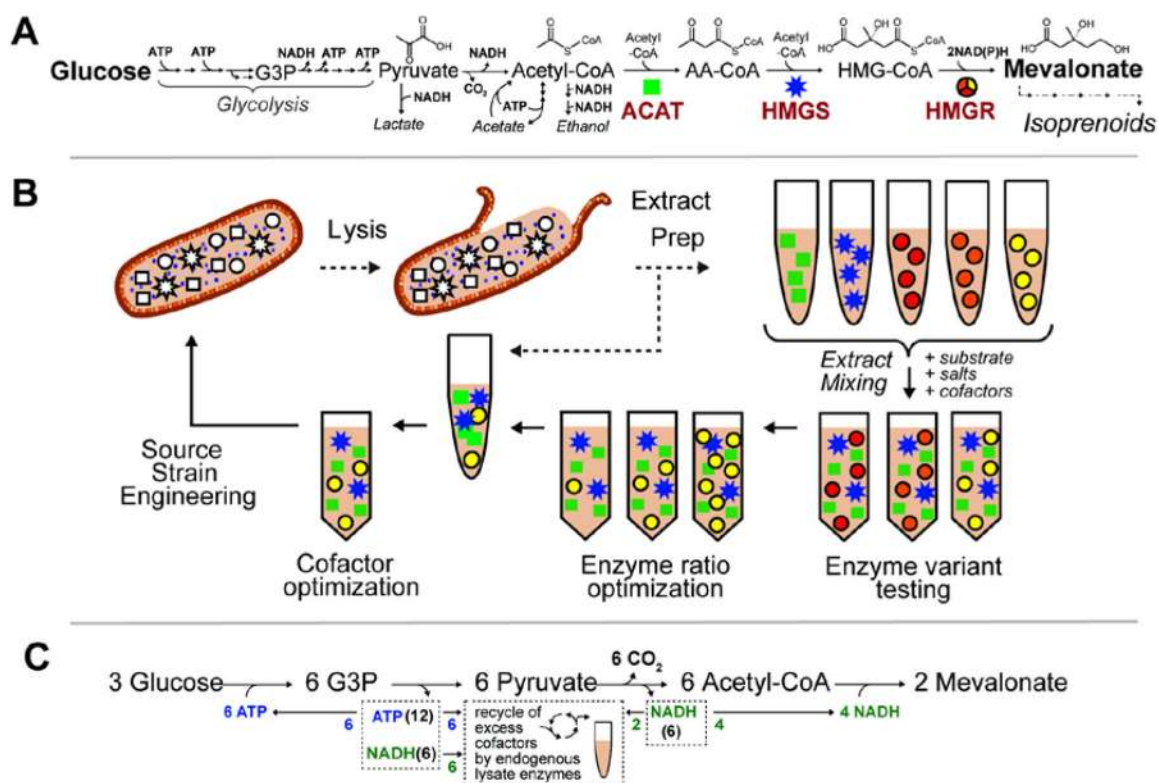
Figure 1. A cell-free metabolic engineering (CFME) framework for pathway prototyping demonstrated with the mevalonate pathway.

(A) Enzymatic route for isoprenoid synthesis via the mevalonate pathway. Acetyl-CoA acetyltransferase (ACAT, green square), hydroxymethylglutaryl-CoA synthase (HMGS, blue star), and hydroxymethylglutaryl-CoA reductase (HMGR, yellow circle) are selectively overexpressed in *E. coli* prior to cell lysis and extract preparation. (B) Cell-free metabolic engineering approach. *E. coli* containing overexpressed enzymes of the mevalonate pathway are lysed and centrifuged to make multiple distinct crude extracts. Mixing of extracts allows testing of enzyme variants and optimization of enzyme ratios; subsequently, cofactors such as ATP, NAD$^+$, and CoA can be optimized and genomic modifications made to the source strain. (C) Pathway balancing. Three glucose can be converted to two mevalonate assuming non-pathway enzymes in the lysate convert 6 excess ATP and 8 excess NADH to ADP and NAD$^+$, respectively.
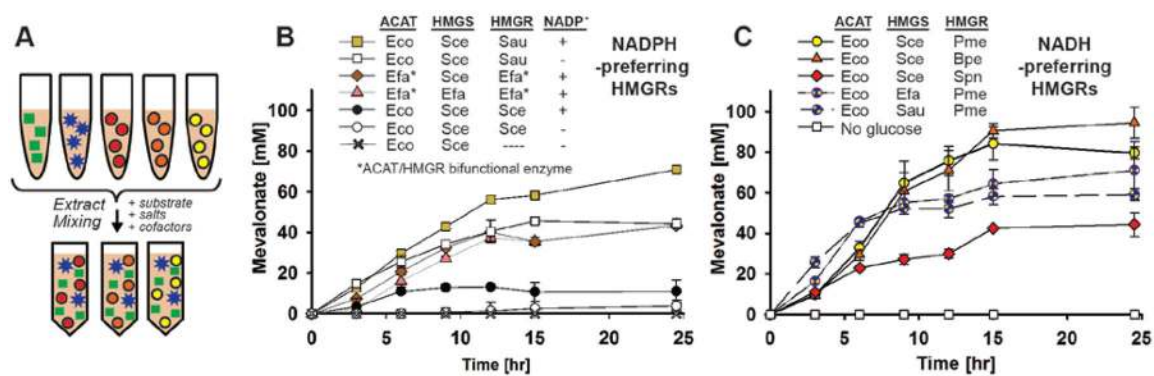
Figure 2. Synthesis of mevalonate from glucose via mixing of three BL21(DE3) extracts each containing a single overexpressed pathway enzyme (ACAT, HMGS, or HMGR), plus native glycolysis enzymes

(**A**). Enzyme variant prototyping identified active NADPH-preferring HMG-CoA reductases (B), but demonstrated that NADH-dependent reductases (C) produced a higher mevalonate titer. Each extract contributed 3.3 mg·mL^{-1} of total protein to the reaction. The system containing ACAT from *E. coli*, HMGS from *S. cerevisiae*, and HMGR from *P. mevalonii* was selected for future characterization. Values represent averages (n=3) and error bars represent 1 s.d.
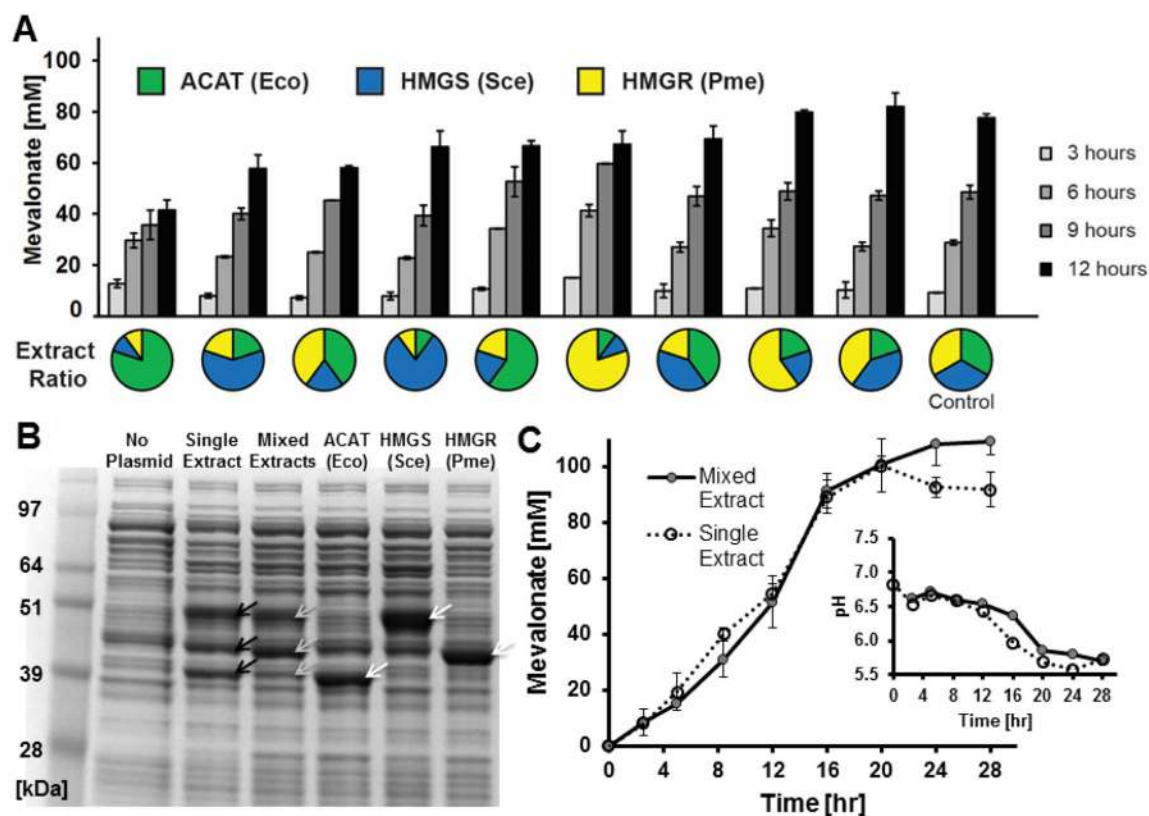
Figure 3. Modulating extract ratios informs construction of an all-in-one extract.
(A) Varying the mass ratio of the three extracts demonstrates expression of pathway
enzymes is not rate-limiting to the system. (B) SDS-PAGE gel (Coomassie stain) shows:
overexpression of three pathway enzymes in a single extract, individual enzyme-enriched
extracts mixed together in a CFME reaction, and individual enzyme-enriched extracts. (C)
The single BL21(DE3) extract with all three pathway enzymes overexpressed performs
similarly to three extracts mixed at equal ratios (Insert) Enzymes are active though pH
decreases over the course of reaction. Addition of buffers stabilizes the pH but does not
affect mevalonate yield. Values represent averages (n=2 for A, n=3 for C) and error bars
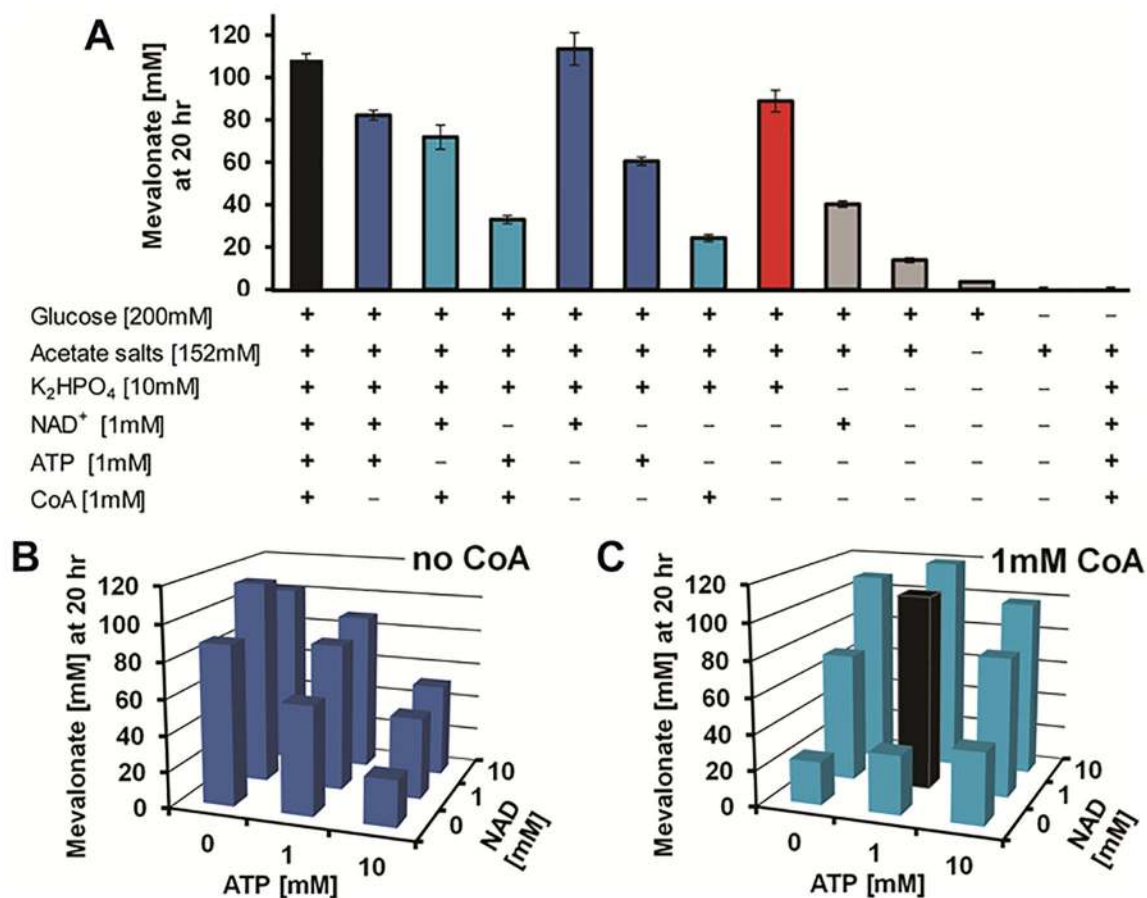represent 1 s.d.

Figure 4. The presence of and concentration of cofactors modulates mevalonate yield.
(A) Cofactors NAD^{+}, ATP, and CoA were supplemented to the reaction two-at-a-time, one-at-a-time, and not supplemented at all. Glucose, acetate salts, phosphate, and extract can support ~80% of yield with no supplementary cofactors (red bar). Variation of initial ATP and NAD^{+} concentration with no CoA (B) and 1mM CoA (C) modulates final mevalonate concentration at 20 hours. The black bar in (A) and (C) represents the cofactor concentration (1 mM ATP, 1 mM NAD^{+}, 1 mM CoA) used in all other figures. Values represent averages (n=3) and error bars represent 1 s.d.
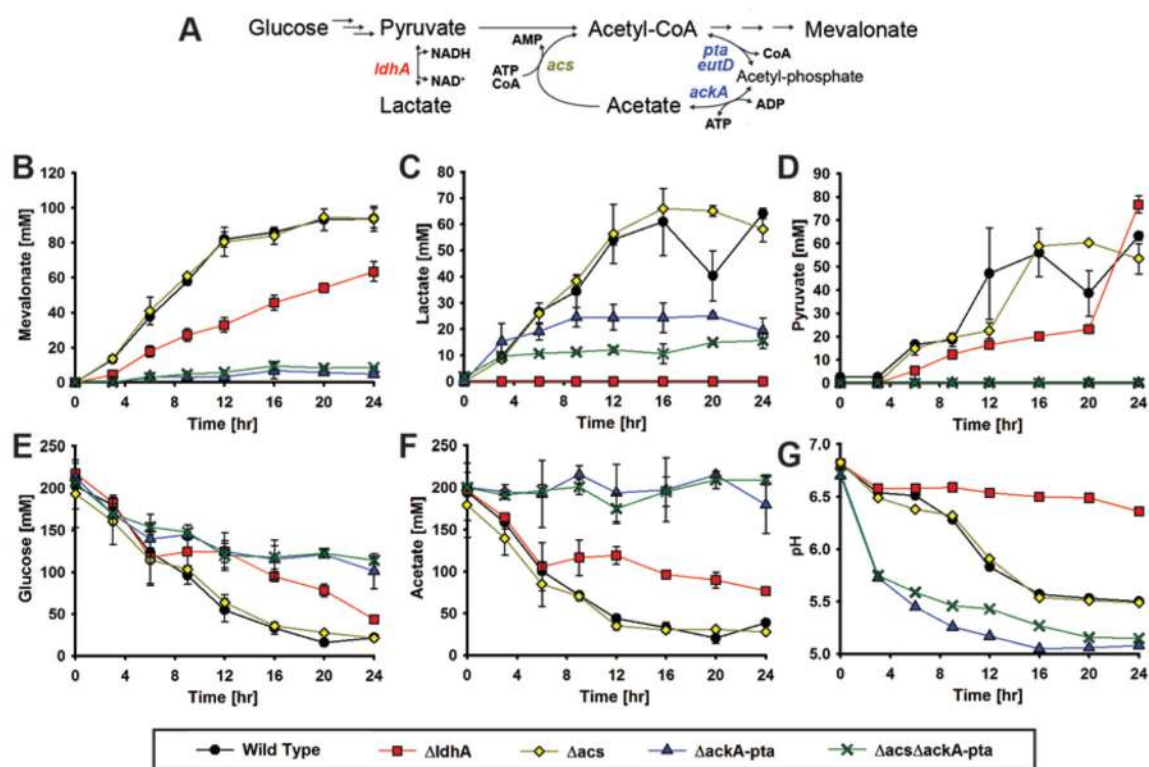
Figure 5. Source strain genome engineering can redirect metabolic flux in the cell free reaction.
(A) Simplified metabolic pathway with target enzymes for knockout in color. (B-G)
Concentrations of metabolites over time within a cell free reaction: (B) Mevalonate (C)
Lactate (D) Pyruvate (E) Glucose (F) Acetate (G) pH. Knockout of *ldhA* eliminates lactate
accumulation and knockout of *ackA-pta* eliminates acetate consumption. Values represent
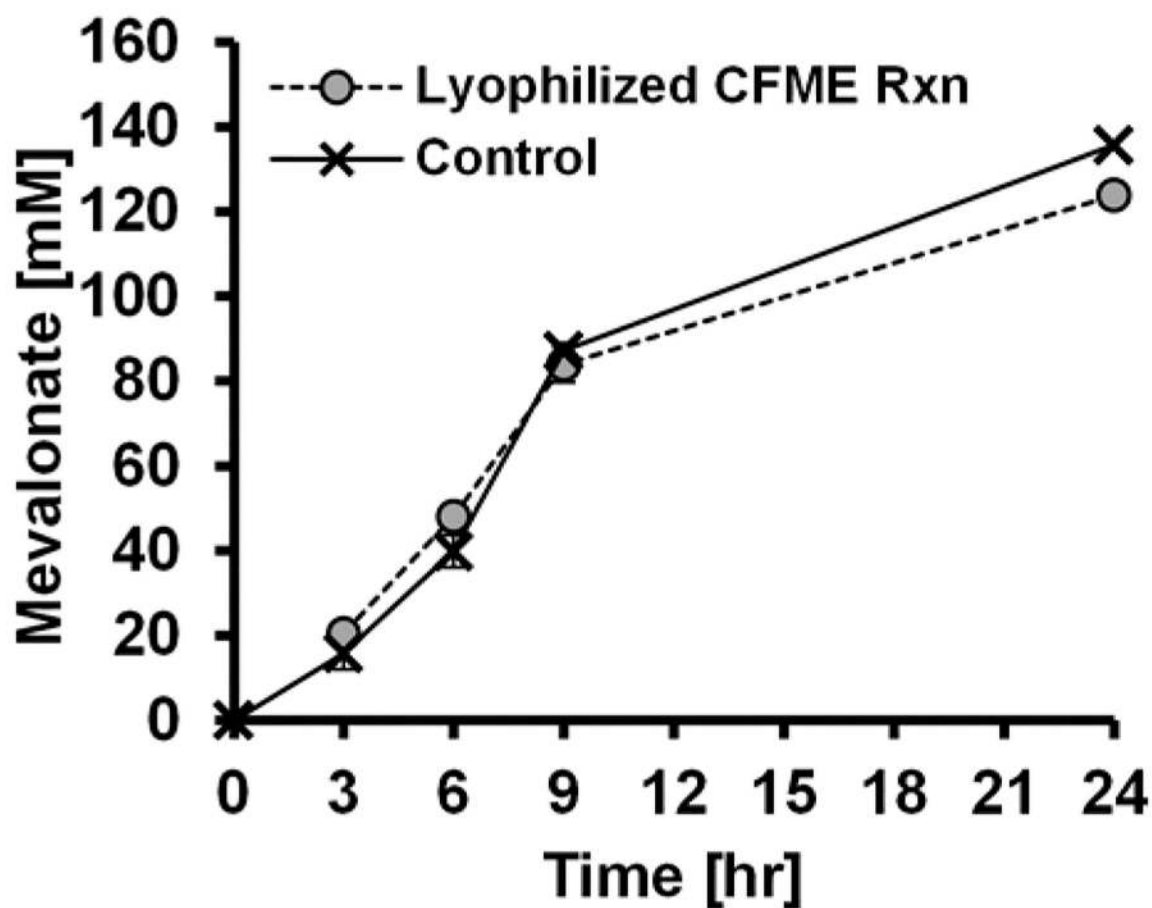averages (n=3) and error bars represent 1 s.d.

Figure 6. Lyophilization of cell-free reactions for mevalonate production.
Complete CFME reactions containing the enzyme-enriched lysate, substrates, cofactors and salts were assembled, immediately flash-frozen, and lyophilized. The rehydrated reactions generated similar mevalonate synthesis rates and titers compared to the control non-freeze dried system. Values represent averages (n=3) and error bars represent 1 s.d.

Table 1.

Strains and plasmids used in this study.

E. coli Strains	Description	Source	
BL21(DE3)	*fhuA2 [lon] ompT gal (λ DE3) [dcm] ΔhsdS λ DE3 = λ sBamHIo ΔEcoRI-B int:: (lacI::PlacUV5::T7 gene1) i21 Δnin5*	NEB	
BL21(DE3)ΔldhA	BL21(DE3) with ldhA replaced by FRT-containing sequence	This study	
BL21(DE3)Δacs	BL21(DE3) with acs replaced by FRT-containing sequence	This study	
BL21(DE3)ΔackA-pta	BL21(DE3) with ackA-pta replaced by FRT-containing seq.	This study	
BL21(DE3)ΔacsΔackA-pta	BL21(DE3) with acs and ackA-pta replaced by FRT-containing seq.	This study	
Plasmids	**Description / Enzyme name**	**Source Organism**	**Reference**
pET-22b	ColE1(pBR322) ori, lacI, T7lac, Amp^R	-	Novagen/ EMD Millipore
pETBCS	pET-22b (signal sequence removed + modified restriction sites)	-	33
pETBCS-ACAT (Eco)	acetyl-CoA acetyltransferase	*Escherichia coli*	43
pETBCS-HMGS (Sce)	hydroxymethylglutaryl-CoA synthase	*Saccharomyces cerevisiae*	43
pETBCS-HMGS (Efa)	hydroxymethylglutaryl-CoA synthase	*Enterococcus faecalis*	5
pETBCS-HMGS (Sau)	hydroxymethylglutaryl-CoA synthase	*Staphylococcus aureus*	48
pETBCS-HMGR (Sce)	hydroxymethylglutaryl-CoA synthase (NADPH-dependent)	*Saccharomyces cerevisiae*	43
pETBCS-HMGR (Sau)	hydroxymethylglutaryl-CoA reductase (NADPH-preferring)	*Staphylococcus aureus*	48
pETBCS-HMGR (Pme)	hydroxymethylglutaryl-CoA reductase (NADH-dependent)	*Pseudomonas mevalonii*	49
pETBCS-HMGR (Bpe)	hydroxymethylglutaryl-CoA reductase (NADH-dependent)	*Bordetella petrii*	49
pETBCS-HMGR (Spn)	hydroxymethylglutaryl-CoA reductase (NADH-dependent)	*Streptococcus pneumoniae*	50
pETBCS-ACAT_HMGR (Efa)	ACAT and HMGR (NADPH-dep) - bifunctional enzyme	*Enterococcus faecalis*	5
pETBCS-HMGR(Pme)-HMGS(Sce)-ACAT(Eco)	HMGR(Pme), HMGS(Sce), & ACAT(Eco) (in sequence on a single mRNA transcript with unique ribosome binding sites	*P. mevalonii, S. cerevisiae, E. coli*	This study